Magnetic properties of the t-J model in two- and three-dimensional lattices

Zhe Chang*
CCAST (World Laboratory), P.O. Box 8730, 100080 Beijing, China
and Institute of High Energy Physics, Academia Sinica, P.O. Box 918(4), 100039 Beijing, China
(Received 22 July 1997; revised manuscript received 3 September 1997)

Magnetic properties of the t-J model in two- and three-dimensional lattices are investigated by a systematic method. The quasiparticle picture, and in particular, dispersion relations of holons and renormalized spinons are presented explicitly. Results are compared with that of numerical simulations and they are in qualitative agreement. The expression of low-temperature magnetization gives a reasonable explanation for the strange phenomena of doping enhancement of the half-filled antiferromagnetic ground state at low temperatures, which was discovered years ago in neutron-scattering experiments. Features at the phase transition region predict antiferromagnetic-metallic transition and give an expression for the doping-dependent Néel temperature. [S0163-1829(98)06105-0]

I. INTRODUCTION

More than ten years after the discovery of high-temperature superconductivity[1] the nature of the normal state of cuprate materials remains an intriguing and controversial issue. The dc resistivity ρ_{ab} of the hole-doped cuprates is linear with temperature when the dopant density is optimal.[2] The Hall coefficient R_H at constant temperature changes sign as the hole density is increased away from the insulator parent compound.[3] Several theories have been proposed to describe them. Unfortunately, most of the available experimental data are not accurate enough to convincingly confirm or rule out many of the theories. It is possible that theories that combine the pairing ideas with the presence of strong antiferromagnetic correlations may properly describe the high-temperature superconductors.[4–6] The interchange of magnons may produce the attractive force needed to pair the charge carriers.[7,8] Some other theorists strongly believe that the BCS theory[9] cannot work in the high-temperature superconductors. Due to the nature of the phonon-mediated electron-electron interaction in BCS theory, there are upper bounds on the critical temperatures much lower than those achieved with the cuprate compounds. The lack of a significant isotope effect with substitution of the oxygen sites seems to rule out the possibility that the phonon Debye frequency is the characteristic energy scale entering in the fundamental equations of the high-temperature superconductivity. Instead, scenarios in which the elementary excitations in the cuprates are spinons (zero charge, spin-1/2) and holons (charge e, spin 0) have been proposed.[10] Anderson[11] argued that the appropriate model for the high-temperature superconductivity is the single-band Hubbard model[12] in the strong on-site Coulomb repulsion limit. Standard strong-coupling perturbation treatment of the single-band Hubbard Hamiltonian produces the effective t-J model.[13,14] The t-J Hamiltonian is an interesting model on its own. This model can be obtained in the strong-coupling limit from a more realistic model that takes into account the more detailed orbital structure of the CuO_2 cell even when the holes created by doping sit primarily on the oxygen sites.[15] The Hubbard model and the t-J model are believed to represent the gross features of the electronic behavior of the new materials. While band-structure calculations succeed in predicting some features of this unusual electronic state,[16] it is clear that electron correlations play an important role in determining the physical properties of these compounds. As a manifestation of these correlations, magnetic fluctuations have now been detected in neutron-scattering experiments[17] on high-temperature superconductors. The magnetism in the undoped parent compounds of both families is now quite well understood. The system of interacting localized Cu^{2+} spins is well described by the two-dimensional Heisenberg Hamiltonian,[18] and a small coupling between the CuO_2 layers leads to the formation of a three-dimensional Néel-ordered state. It is therefore clearly of great interest to investigate in detail the crossover from the rather conventional local moment system at zero doping to the electronic state that forms the basis for high-temperature superconductivity.

In this paper, we discuss magnetic properties of the high-temperature superconductors as the dopant density is increased away from the insulator parent compound in a whole temperature range by making use of the quantum field theory. The quasiparticle picture, and in particular, dispersion relations for holons and renormalized spinons are presented and discussed in detail. Results are compared with that of numerical simulations and they are in qualitative agreement. The expression of low-temperature magnetization gives a reasonable explanation for the strange phenomena of doping enhancement of the half-filled antiferromagnetic ground state of the high-temperature superconductors at low temperatures, which was discovered years ago in neutron-scattering experiments.[19] Features at the phase-transition region predict an antiferromagnetic-metallic transition and an expression for the doping-dependent Néel temperature is given.

The paper is organized as follows. In Sec. II, we set up a Green's-function formalism of the t-J model within the framework of supergroup theory in two- and three-dimensional lattices. The quasiparticle picture of the high-temperature superconductors, and in particular, dispersion relations for holons and renormalized spinons are discussed in Sec. III. Section IV is devoted to investigating magnetiza-

tion at zero temperature and finite dopant density. At low temperatures, the expression of sublattice magnetization gives a possible explanation for the doping enhancement of the antiferromagnetic ground state of the high-temperature superconductors at low temperatures, which was discovered in neutron-scattering experiments years ago. The magnetic properties of the cuprate materials at low temperatures are discussed in Sec. V. In Sec. VI, features of the t-J model near phase-transition region are investigated and compared with the phase diagram of the realistic high-temperature superconductors. Some concluding remarks are presented in Sec. VII.

II. FORMALISM

There is a great deal of similarity between the quantum field theory and the theories based on statistical mechanics as far as the many-body aspect is concerned. Because of the lack of a systematic method there was little advancement of the many-body theory until the 1950's. The situation has changed greatly since then, the quantum field theory provides a very powerful and unified way of attacking the many-body problem. It is well known that the Green's functions play the most important part in the field-theoretic treatment of the many-body problem. The Green's functions enjoy popularity because they yield, in a direct way, the most important physical properties of a system, having a simple physical interpretation, and can be calculated in a systematic way. In the 1960's, a successful Green's-function approach for the ferromagnetism[20] and antiferromagnetism[21] was developed. Here we would like to set up the Green's-function formalism of the t-J model within the framework of the supergroup theory. To this end, first of all, we rewrite the t-J Hamiltonian into an explicit supersymmetric form. The familiar form of the t-J model is

$$H=-t\sum_{(\mathbf{jk})}\sum_{\sigma}\ (c^{\dagger}_{\mathbf{j}\sigma}c_{\mathbf{k}\sigma}+c^{\dagger}_{\mathbf{k}\sigma}c_{\mathbf{j}\sigma})+J\sum_{(\mathbf{jk})}\left(\mathbf{S}_{\mathbf{j}}\cdot\mathbf{S}_{\mathbf{k}}-\frac{1}{4}\,\delta_{n_{\mathbf{j}}n_{\mathbf{k}}}\right), \tag{1}$$

where the notation is standard.

The Hilbert space of the t-J model is spanned by $|a_{\mathbf{j}}\rangle \in\{|\uparrow_{\mathbf{j}}\rangle(=c^{\dagger}_{\mathbf{j}\uparrow}|0\rangle_{\mathbf{j}}),\ |\downarrow_{\mathbf{j}}\rangle(=c^{\dagger}_{\mathbf{j}\downarrow}|0\rangle_{\mathbf{j}}),\ |0_{\mathbf{j}}\rangle(=|0\rangle_{\mathbf{j}})\}$. With the local states $|a_{\mathbf{j}}\rangle$, one can define the local Hubbard operators $X^{ab}_{\mathbf{j}}\equiv|a_{\mathbf{j}}\rangle\langle b_{\mathbf{j}}|$. The operators $X^{ab}_{\mathbf{j}}$ are generators of the supergroup $U(2/1)$ and satisfy the related superalgebra relation[22]

$$[X^{ac},X^{bd}\}=X^{ad}\delta^{bc}\pm X^{bc}\delta^{ad}. \tag{2}$$

The t-J Hamiltonian in terms of the local Hubbard operators $X^{ab}_{\mathbf{j}}$ is of the form

$$H=-t\sum_{\langle\mathbf{jk}\rangle}\sum_{\sigma}\ (X^{\sigma 0}_{\mathbf{j}}X^{0\sigma}_{\mathbf{k}}+X^{\sigma 0}_{\mathbf{k}}X^{0\sigma}_{\mathbf{j}})+\frac{J}{2}\sum_{\langle\mathbf{jk}\rangle}\sum_{\sigma,\sigma'}X^{\sigma\sigma'}_{\mathbf{j}}X^{\sigma'\sigma}_{\mathbf{k}}$$
$$-\frac{J}{2}\sum_{\langle\mathbf{jk}\rangle}X^{00}_{\mathbf{j}}X^{00}_{\mathbf{k}}. \tag{3}$$

It is convenient to present the generators $X^{ab}_{\mathbf{j}}$ in terms of a boson and a fermion operator, which denotes magnon and hole excitations, respectively. This is given by the general Holstein-Primakoff transformation.[23]

To connect the Green's functions of supergroup generators with sublattice magnetization, we notice the Casimir operator of the supergroup $U(2/1)$. This is the only supersymmetric invariant quantity of the formalism. The Casimir operator $\mathcal{C}$ of the supergroup $U(2/1)$ is as follows:

$$\mathcal{C}=X^{\uparrow\uparrow}_{\mathbf{j}}X^{\uparrow\uparrow}_{\mathbf{j}}+X^{\uparrow\downarrow}_{\mathbf{j}}X^{\downarrow\uparrow}_{\mathbf{j}}+X^{\downarrow\uparrow}_{\mathbf{j}}X^{\uparrow\downarrow}_{\mathbf{j}}+X^{\downarrow\downarrow}_{\mathbf{j}}X^{\downarrow\downarrow}_{\mathbf{j}}+(X^{0\uparrow}_{\mathbf{j}}X^{\uparrow 0}_{\mathbf{j}}-X^{\uparrow 0}_{\mathbf{j}}X^{0\uparrow}_{\mathbf{j}}$$
$$+X^{0\downarrow}_{\mathbf{j}}X^{\downarrow 0}_{\mathbf{j}}-X^{\downarrow 0}_{\mathbf{j}}X^{0\downarrow}_{\mathbf{j}})-X^{00}_{\mathbf{j}}X^{00}_{\mathbf{j}}. \tag{4}$$

It is too complicated to discuss the above Casimir operator directly. In fact, here we only interested in the fundamental representation of the supergroup $U(2/1)$. In this case, we have identities

$$X^{00}_{\mathbf{j}}+X^{\uparrow\uparrow}_{\mathbf{j}}+X^{\downarrow\downarrow}_{\mathbf{j}}\equiv 1,$$

$$X^{\uparrow 0}_{\mathbf{j}}X^{0\uparrow}_{\mathbf{j}}+X^{\downarrow 0}_{\mathbf{j}}X^{0\downarrow}_{\mathbf{j}}\equiv 1-X^{00}_{\mathbf{j}}. \tag{5}$$

Thus, a simplified form of the Casimir operator $\mathcal{C}$ is obtained,

$$\mathcal{C}=2X^{\uparrow\downarrow}_{\mathbf{j}}X^{\uparrow\downarrow}_{\mathbf{j}}+X^{00}_{\mathbf{j}}+(X^{\uparrow\uparrow}_{\mathbf{j}}-X^{\downarrow\downarrow}_{\mathbf{j}}). \tag{6}$$

And then the magnetization S^3 can be written in terms of local Hubbard operators

$$S^3=\frac{\mathcal{C}}{2}-\frac{1}{2}\,X^{00}_{\mathbf{j}}-X^{\downarrow\uparrow}_{\mathbf{j}}X^{\uparrow\downarrow}_{\mathbf{j}}. \tag{7}$$

Therefore, after obtaining the correlation function $\langle X^{\downarrow\uparrow}_{\mathbf{j}}X^{\uparrow\downarrow}_{\mathbf{j}}\rangle$, we got directly the sublattice magnetization. It is well known that the correlation function can be calculated effectively by using the analytical properties of the double times Green's function $\langle\langle X^{\uparrow\downarrow}_{\mathbf{j}}(\tau);X^{\downarrow\uparrow}_{\mathbf{j}}(\tau')\rangle\rangle$. Thus, to calculate the magnetization it is transformed as to get the Green's function $\langle\langle X^{\uparrow\downarrow}_{\mathbf{j}}(\tau);X^{\downarrow\uparrow}_{\mathbf{j}}(\tau')\rangle\rangle$. In this paper, we calculate the Green's function by solving equations of motion of the Green's function.

We consider a simple lattice. To make the problem tractable, we divide the lattice into ''A'' and ''B'' sublattices. For the bipartite lattice, $\mathbf{j_1}$ and $\mathbf{j_1}+\boldsymbol{\delta}$ are on different sublattice and consequently have two different Green's functions. Using the ''Tyablikov'' decoupling procedure,[24] from the Heisenberg equations, one gets the equations of motion in the Green's functions

$$i\frac{d}{d\tau}\langle\langle X^{\uparrow\downarrow}_{\mathbf{j}_1}(\tau);X^{\downarrow\uparrow}_{\mathbf{k}_1}(\tau')\rangle\rangle=\delta(\tau-\tau')2\langle S^3\rangle\delta_{\mathbf{j}_1\mathbf{k}_1}-t\sum_{\boldsymbol{\delta}}\left[\langle\langle X^{\uparrow 0}_{\mathbf{j}_1}(\tau)X^{0\downarrow}_{\mathbf{j}_1+\boldsymbol{\delta}}(\tau);X^{\downarrow\uparrow}_{\mathbf{k}_1}(\tau')\rangle\rangle+\langle\langle X^{0\downarrow}_{\mathbf{j}_1}(\tau)X^{\uparrow 0}_{\mathbf{j}_1+\boldsymbol{\delta}}(\tau);X^{\downarrow\uparrow}_{\mathbf{k}_1}(\tau')\rangle\rangle\right]$$

$$+J\langle S^3\rangle\sum_{\boldsymbol{\delta}}\left[\langle\langle X^{\uparrow\downarrow}_{\mathbf{j}_1+\boldsymbol{\delta}}(\tau);X^{\downarrow\uparrow}_{\mathbf{k}_1}(\tau')\rangle\rangle+\langle\langle X^{\uparrow\downarrow}_{\mathbf{j}_1}(\tau);X^{\downarrow\uparrow}_{\mathbf{k}_1}(\tau')\rangle\rangle\right] \tag{8}$$

and

$$i\frac{d}{d\tau}\langle\langle X^{\uparrow\downarrow}_{\mathbf{j}_1+\boldsymbol{\delta}}(\tau);X^{\downarrow\uparrow}_{\mathbf{k}_1}(\tau')\rangle\rangle=-t\sum_{\boldsymbol{\delta}_1}\left[\langle\langle X^{\uparrow 0}_{\mathbf{j}_1+\boldsymbol{\delta}}(\tau)X^{0\downarrow}_{\mathbf{j}_1+\boldsymbol{\delta}+\boldsymbol{\delta}_1}(\tau);X^{\downarrow\uparrow}_{\mathbf{k}_1}(\tau')\rangle\rangle+\langle\langle X^{0\downarrow}_{\mathbf{j}_1+\boldsymbol{\delta}}(\tau)X^{\uparrow 0}_{\mathbf{j}_1+\boldsymbol{\delta}+\boldsymbol{\delta}_1}(\tau);X^{\downarrow\uparrow}_{\mathbf{k}_1}(\tau')\rangle\rangle\right]$$

$$-J\langle S^3\rangle\sum_{\boldsymbol{\delta}_1}\left[\langle\langle X^{\uparrow\downarrow}_{\mathbf{j}_1+\boldsymbol{\delta}+\boldsymbol{\delta}_1}(\tau);X^{\downarrow\uparrow}_{\mathbf{k}_1}(\tau')\rangle\rangle+\langle\langle X^{\uparrow\downarrow}_{\mathbf{j}_1+\boldsymbol{\delta}}(\tau);X^{\downarrow\uparrow}_{\mathbf{k}_1}(\tau')\rangle\rangle\right]. \tag{9}$$

To make the set of coupled equations of motion in the Green's function self-contained, we have to add the following ones:

$$i\frac{d}{d\tau}\langle\langle X^{\uparrow 0}_{\mathbf{j}_1}(\tau)X^{0\downarrow}_{\mathbf{j}_1+\boldsymbol{\delta}}(\tau);X^{\downarrow\uparrow}_{\mathbf{k}_1}(\tau')\rangle\rangle=-t\langle X^{0\uparrow}_{\mathbf{j}_1}X^{\uparrow 0}_{\mathbf{j}_1}\rangle[\langle\langle X^{\uparrow\downarrow}_{\mathbf{j}_1}(\tau);X^{\downarrow\uparrow}_{\mathbf{k}_1}(\tau')\rangle\rangle-\langle\langle X^{\uparrow\downarrow}_{\mathbf{j}_1+\boldsymbol{\delta}}(\tau);X^{\downarrow\uparrow}_{\mathbf{k}_1}(\tau')\rangle\rangle], \tag{10}$$

$$i\frac{d}{d\tau}\langle\langle X^{0\downarrow}_{\mathbf{j}_1}(\tau)X^{\uparrow 0}_{\mathbf{j}_1+\boldsymbol{\delta}}(\tau);X^{\downarrow\uparrow}_{\mathbf{k}_1}(\tau')\rangle\rangle=-t\langle X^{0\downarrow}_{\mathbf{j}_1}X^{\downarrow 0}_{\mathbf{j}_1}\rangle[\langle\langle X^{\uparrow\downarrow}_{\mathbf{j}_1}(\tau);X^{\downarrow\uparrow}_{\mathbf{k}_1}(\tau')\rangle\rangle-\langle\langle X^{\uparrow\downarrow}_{\mathbf{j}_1+\boldsymbol{\delta}}(\tau);X^{\downarrow\uparrow}_{\mathbf{k}_1}(\tau')\rangle\rangle] \tag{11}$$

and

$$i\frac{d}{d\tau}\langle\langle X^{\uparrow 0}_{\mathbf{j}_1+\boldsymbol{\delta}}(\tau)X^{0\downarrow}_{\mathbf{j}_1+\boldsymbol{\delta}+\boldsymbol{\delta}'}(\tau);X^{\downarrow\uparrow}_{\mathbf{k}_1}(t')\rangle\rangle=-t\langle X^{0\downarrow}_{\mathbf{j}_1}X^{\downarrow 0}_{\mathbf{j}_1}\rangle\sum_{\boldsymbol{\delta}_2}\left[\langle\langle X^{\uparrow\downarrow}_{\mathbf{j}_1+\boldsymbol{\delta}}(\tau);X^{\downarrow\uparrow}_{\mathbf{k}_1}(\tau')\rangle\rangle-\langle\langle X^{\uparrow\downarrow}_{\mathbf{j}_1+\boldsymbol{\delta}+\boldsymbol{\delta}'}(\tau);X^{\downarrow\uparrow}_{\mathbf{k}_1}(\tau')\rangle\rangle\right], \tag{12}$$

$$i\frac{d}{d\tau}\langle\langle X^{0\downarrow}_{\mathbf{j}_1+\boldsymbol{\delta}}(\tau)X^{\uparrow 0}_{\mathbf{j}_1+\boldsymbol{\delta}+\boldsymbol{\delta}'}(\tau);X^{\downarrow\uparrow}_{\mathbf{k}_1}(t')\rangle\rangle=-t\langle X^{0\uparrow}_{\mathbf{j}_1}X^{\uparrow 0}_{\mathbf{j}_1}\rangle[\langle\langle X^{\uparrow\downarrow}_{\mathbf{j}_1+\boldsymbol{\delta}}(\tau);X^{\downarrow\uparrow}_{\mathbf{k}_1}(\tau')\rangle\rangle-\langle\langle X^{\uparrow\downarrow}_{\mathbf{j}_1+\boldsymbol{\delta}+\boldsymbol{\delta}'}(\tau);X^{\downarrow\uparrow}_{\mathbf{k}_1}(\tau')\rangle\rangle]. \tag{13}$$

Translational invariance dictates consideration of the spatial Fourier transforms

$$\langle\langle X^{\uparrow\downarrow}_{\mathbf{j}_1};X^{\downarrow\uparrow}_{\mathbf{k}_1}\rangle\rangle=\frac{2}{N}\sum_{\mathbf{k}}g_{\mathbf{k}}(E)e^{i\mathbf{k}\cdot(\mathbf{j}_1-\mathbf{k}_1)},$$

$$\langle\langle X^{\uparrow\downarrow}_{\mathbf{j}_1+\boldsymbol{\delta}};X^{\downarrow\uparrow}_{\mathbf{k}_1}\rangle\rangle=\frac{2}{N}\sum_{\mathbf{k}}f_{\mathbf{k}}(E)e^{i\mathbf{k}\cdot(\mathbf{j}_1+\boldsymbol{\delta}-\mathbf{k}_1)}, \tag{14}$$

where $\langle\langle X^{\uparrow\downarrow}_{\mathbf{j}_1};X^{\downarrow\uparrow}_{\mathbf{k}_1}\rangle\rangle$ and $\langle\langle X^{\uparrow\downarrow}_{\mathbf{j}_1+\boldsymbol{\delta}};X^{\downarrow\uparrow}_{\mathbf{k}_1}\rangle\rangle$ are the Fourer transforms of the Green's functions $\langle\langle X^{\uparrow\downarrow}_{\mathbf{j}_1}(\tau);X^{\downarrow\uparrow}_{\mathbf{k}_1}(\tau')\rangle\rangle$ and $\langle\langle X^{\uparrow\downarrow}_{\mathbf{j}_1\boldsymbol{\delta}}(\tau);X^{\downarrow\uparrow}_{\mathbf{k}_1}(\tau')\rangle\rangle$, respectively.

Equations (8)–(13) then imply

$$(E^2-Jz\langle S^3\rangle E-t^2z\langle X^{0\uparrow}_{\mathbf{j}_1}X^{\uparrow 0}_{\mathbf{j}_1}+X^{0\downarrow}_{\mathbf{j}_1}X^{\downarrow 0}_{\mathbf{j}_1}\rangle)g_{\mathbf{k}}(E)-(J\langle S^3\rangle E-t^2\langle X^{0\uparrow}_{\mathbf{j}_1}X^{\uparrow 0}_{\mathbf{j}_1}+X^{0\downarrow}_{\mathbf{j}_1}X^{\downarrow 0}_{\mathbf{j}_1}\rangle)z\gamma(\mathbf{k})f_{\mathbf{k}}(E)=2\langle S^3\rangle E, \tag{15}$$

$$(E^2+Jz\langle S^3\rangle E-t^2z\langle X^{0\uparrow}_{\mathbf{j}_1}X^{\uparrow 0}_{\mathbf{j}_1}+X^{0\downarrow}_{\mathbf{j}_1}X^{\downarrow 0}_{\mathbf{j}_1}\rangle)f_{\mathbf{k}}(E)-(-J\langle S^3\rangle E+t^2\langle X^{0\uparrow}_{\mathbf{j}_1}X^{\uparrow 0}_{\mathbf{j}_1}+X^{0\downarrow}_{\mathbf{j}_1}X^{\downarrow 0}_{\mathbf{j}_1}\rangle)z\gamma(\mathbf{k})g_{\mathbf{k}}(E)=0 \tag{16}$$

or

$$g_{\mathbf{k}}(E)=\frac{2\langle S^3\rangle E(E^2+Jz\langle S^3\rangle E-2t^2z\langle f^{\dagger}f\rangle)}{E^4+[4t^2z\langle f^{\dagger}f\rangle+J^2\langle S^3\rangle^2z^2(1-\gamma^2(\mathbf{k}))]E^2+4t^4z^2(1-\gamma^2(\mathbf{k}))\langle f^{\dagger}f\rangle^2}, \tag{17}$$

where we have used the notation $\gamma(\mathbf{k})=1/z\Sigma_{\delta}e^{i\mathbf{k}\cdot\delta}$, z is the number of nearest neighbors. Now, we can say that a systematic Green's-function formalism of the t-J model is already set up. Magnetic properties of the high-temperature superconductors can be discussed straightforwardly using the method. However, before investigating of the magnetic properties, we first try to gain some insights of the quasiparticle picture of the t-J model in the following section.

III. QUASIPARTICLE PICTURE

It is believed that the physics of the half-filled limit is mostly understood. The situation, where carriers are added, is more challenging and interesting. The study for a few holes in an antiferromagnetic background is an important topic in the study of the high-temperature superconductivity. One of the most controversial issues in the context is whether a hole injected in the undoped ground state behaves like a quasiparticle. Based on results obtained in the one-dimensional Hubbard model, Anderson[25] proposed a scenario where the spinons heavily address the holes, increasing substantially the mass; this renormalization is so strong that the wave-function renormalization at the Fermi surface vanishes. However, this is a very particular situation caused by the dimensionality of the problem.

To discuss the quasiparticle picture, we rewrite $g_{\mathbf{k}}(E)$ in the following form:

$$g_{\mathbf{k}}(E)=\frac{2\langle S^3\rangle E(E^2+J\langle S^3\rangle zE-2t^2z\langle f^{\dagger}f\rangle)}{(E+E_h)(E-E_h)(E+E_s)(E-E_s)}, \tag{18}$$

where the $E_{h(s)}$ dispersion relation of holons (renormalized spinons), is of the form

$$E_h(\mathbf{k})=-\frac{1}{\sqrt{2}}\sqrt{\varepsilon^2(\mathbf{k})-\sqrt{\varepsilon^4(\mathbf{k})-16t^4z^2(\langle f^{\dagger}f\rangle)^2(1-\gamma^2(\mathbf{k}))}}$$

$$E_s(\mathbf{k})=\frac{1}{\sqrt{2}}\sqrt{\varepsilon^2(\mathbf{k})+\sqrt{\varepsilon^4(\mathbf{k})-16t^4z^2(\langle f^{\dagger}f\rangle)^2(1-\gamma^2(\mathbf{k}))}}. \tag{19}$$

Here $\varepsilon(\mathbf{k})\equiv\sqrt{J^2\langle S^3\rangle^2z^2(1-\gamma^2(\mathbf{k}))+4t^2z\langle f^{\dagger}f\rangle}$.

And then, we can write $g_{\mathbf{k}}(E)$ as

$$\begin{aligned}g_{\mathbf{k}}(E)=&\langle S^3\rangle\frac{1}{E_h^2-E_s^2}\left[\frac{E_h^2+J\langle S^3\rangle zE_h-2t^2z\langle f^{\dagger}f\rangle}{E-E_h}\right.\\&\left.+\frac{E_h^2-J\langle S^3\rangle zE_h-2t^2z\langle f^{\dagger}f\rangle}{E+E_h}\right]\\&+\langle S^3\rangle\frac{1}{E_s^2-E_h^2}\left[\frac{E_s^2+J\langle S^3\rangle zE_s-2t^2z\langle f^{\dagger}f\rangle}{E-E_s}\right.\\&\left.+\frac{E_s^2-J\langle S^3\rangle zE_s-2t^2z\langle f^{\dagger}f\rangle}{E+E_s}\right].\end{aligned} \tag{20}$$

It is within our expectation that there are four poles of the $g_{\mathbf{k}}(E)$. The first two, $E\pm E_h$, correspond to the quasihole excitations, and the other two poles, $E\pm E_s$, denote the renormalized spinons.

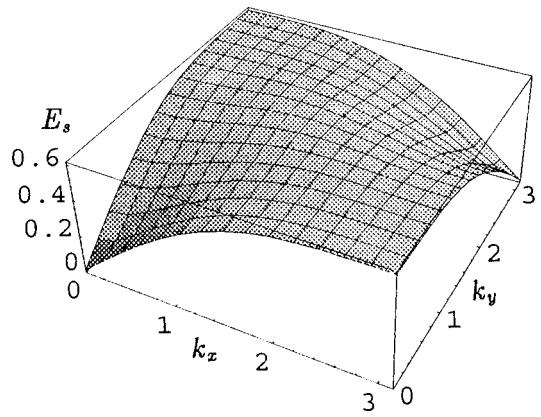

FIG. 1. Spinon dispersion surface plotted in the Brillouin zone, for a 2D square lattice with lattice parameter $a=1$, for the half-filling case, for $t=1$, $J=0.3$.

As the dopant density is increased away from the insulator parent compound, the magnetic properties of the high-temperature superconductors are less understood, though they are more interesting than the half-filling limit. Several theoretical works have studied the degree of suppression of antiferromagnetism by addition of holes to the t-J model or Hubbard model at half-filling. Dagotto *et al.*[26] calculated the dynamical spin structure function $S(\mathbf{Q},\omega)$ $[\mathbf{Q}=(\pi,\pi)]$ for the t-J model on a 4×4 cluster at $J/t=0.4$, and several dopings. Their results show a sharp peak at low frequencies and doping corresponding to the spin-wave excitation which, at half-filling and in the bulk limit, becomes massless. The finite size of the cluster, plus the effect of doping, opens a gap in the spectrum corresponding to this momentum. For $\delta=0.25$, a considerable amount of spectral weight is transferred to large energies. For the quarter-filled system, the spin-wave peak has virtually disappeared. Here, by making use of the Green's-function method, we got a reasonable general expression for the dispersion relation of the renormalized spinons. From the dispersion relation, we can obtain the same conclusion with these numerical simulations. It should be noticed that the dispersion relation for the renormalized spinons, in the case of low doping, is of the form

$$E=\sqrt{J^2\langle S^3\rangle^2z^2(1-\gamma^2)+4t^2z\langle f^{\dagger}f\rangle}. \tag{21}$$

At the exact half-filling case, the correct dispersion relation (massless) for the spinons is reduced. And it is the finite doping, which generates a nonzero effective mass for the spinons.

Evolution of the renormalized spinon's dispersion relation with rising doping concentration ($\langle f^{\dagger}f\rangle$) can be viewed from Figs. 1–3. Figure 1 shows a linear dispersion relation for massless spinons at low frequencies, this corresponding to the half-filling case. From Fig. 2, we can see that an effective mass of the renormalized spinons is generated by finite doping. And Fig. 3 presents a more general picture of the dispersion relation in the two-dimensional lattice.

The study for motions of a few holes in an antiferromagnetic background were carried out mainly using numerical methods, with the help of some analytical techniques. To gain some intuition on the behavior of holes doped into an antiferromagnet, one always starts with the study of just one hole. The physics of a hole arises from a competition be-

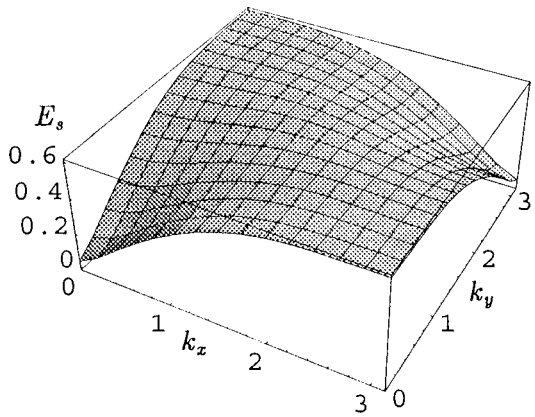

FIG. 2. Spinon dispersion surface plotted in the Brillouin zone, for a 2D square lattice with lattice parameter $a=1$, for doping concentration ($\langle f^{\dagger}f\rangle=$)0.0001, for $t=1$, $J=0.3$.

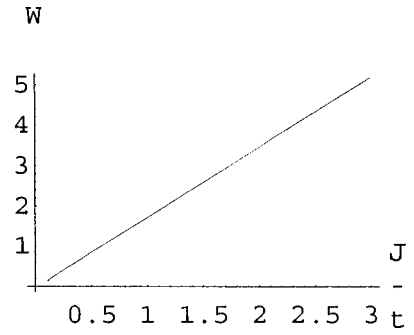

FIG. 4. Bandwidth W of the t-J model as a function of J/t, for $t=1$, for dopant density $\langle f^{\dagger}f\rangle=1/1600$.

tween the superexchange energy lost near the hole and its kinetic energy. It is reasonable to expect that the antiferromagnetic order parameter will reduce its magnitude near the hole, increasing the mobility of the carrier inside such a spin bag. The effects of a so-called string linear potential strongly influence the physics of holes in antiferromagnets.[27] For the particular case of one hole in antiferromagnet, analytical approaches have been developed that give results in good agreement with exact diagonalization predictions. Assuming that the weight beyond the first pole was incoherent and using the slave-boson or general Holstein-Primakoff transformation and the $1/S$ expansion, at the dominant pole approximation, the single-particle Green's function of one hole was studied.[28–30] The self-consistent Born approximation to this reformulated problem was also studied.[31] This is equivalent to the rainbow approximation for the holon propagator, where the spinon lines are noncrossing. A remarkable agreement with exact diagonalization results was found for small J/t. Unfortunately, an extension of this approach to a finite density of holes is difficult.

By making use of the quantum field theory, we now obtain a general expression for the dispersion relation of the holons. Its total bandwidth W provides information about the renormalization effects caused by the spin waves that are created and absorbed while the hole propagates. Moreover, if the normal state is assumed to be formed by a gas with noninteracting (spin-wave renormalized) holes, then a lot of observables can be calculated. In addition, the specific $\mathbf{k}$ dependence of the energy provides information about anisotropies in the system. In Fig. 4, the bandwidth W, which is defined as the difference between the energy of the state with the minimum energy and of the state with highest energy, is plotted as a function of J/t. We see that the bandwidth seems proportional to J/t. This result is in good agreement with other calculations[28–32] and numerical simulations[33] for a hole in antiferromagnets. In Fig. 5, we present a hole dispersion curve plotted along the direction $\Gamma MX\Gamma$ in the Brillouin zone. This result is also in agreement with numerical ones using a Green's function Monte Carlo method and the Born approximation[34] (see Fig. 13 in Ref. 34). An interesting feature of Fig. 5 is the degeneracy between momentum $\mathbf{k}=(\pi/2,\pi/2)$ and $\mathbf{k}=(0,\pi),(\pi,0)$. Analyzed from the point of view of the Hubbard model, this is not surprising, since in the noninteracting limit both momenta belong to the Fermi surface, thus at least at weak coupling, only a tiny splitting in energy is expected. However, the Born approximation and numerical simulation using a Green's-function Monte Carlo method show a small difference in energy between $\mathbf{k}=(\pi/2,\pi/2)$ and $\mathbf{k}=(0,\pi),(\pi,0)$. According to Dagotto *et al.*, it is the small fraction of difference forming the basis for a possible explanation of the behavior of the Hall coefficient with temperature in the high-temperature superconductors.

To gain more information, in Figs. 6 and 7, we present a three-dimensional surface plot and a contour plot of the

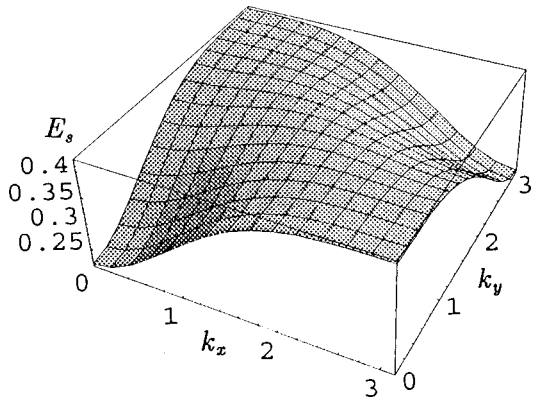

FIG. 3. Spinon dispersion surface plotted in the Brillouin zone, for a 2D square lattice with lattice parameter $a=1$, for doping concentration ($\langle f^{\dagger}f\rangle=$)0.003, for $t=1$, $J=0.3$.

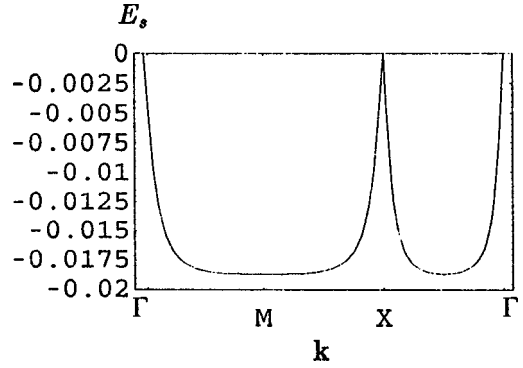

FIG. 5. Hole dispersion curve plotted along the direction $\Gamma(0,0)M(\pi,0)X(\pi,\pi)\Gamma(0,0)$ in the Brillouin zone, for a 2D square lattice with lattice parameter $a=1$, for doping concentration ($\langle f^{\dagger}f\rangle=$)0.001, for $t=1$, $J=0.3$.

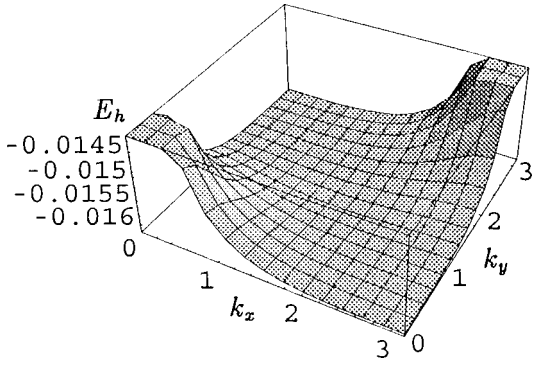

FIG. 6. Hole dispersion surface plotted in the Brillouin zone, for a 2D square lattice with lattice parameter $a=1$, for doping concentration ($\langle f^{\dagger}f\rangle=$)0.001, for $t=1$, $J=0.3$.

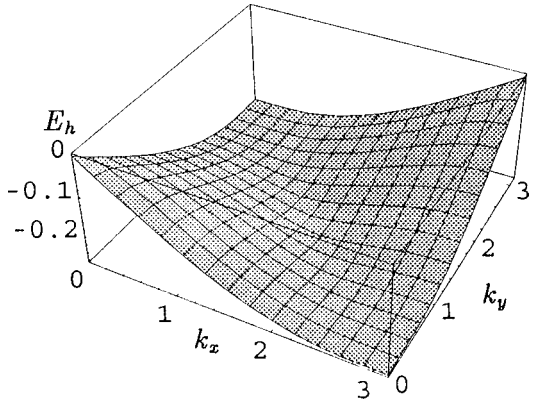

FIG. 8. Hole dispersion surface plotted in the Brillouin zone, for a 2D square lattice with lattice parameter $a=1$, for doping concentration ($\langle f^{\dagger}f\rangle=$)0.01, for $t=1$, $J=0.3$.

hole's dispersion relation. Comparison of Figs. 8 and 9 with Figs. 6 and 7 gives insight into the evolution process of the hole's dispersion relation with rising doping concentration. These results show that the rapid reduction of antiferromagnetism with doping can be mimicked by the quasiparticle picture.

IV. MAGNETIZATION AT ZERO TEMPERATURE

It is believed that undoped cuprate materials are described by the two-dimensional Heisenberg lattice. It is well established from numerical work (quantum Monte Carlo, Green's-function Monte Carlo, series analysis) and different variational methods that the ground state of the two-dimensional $S=1/2$ Heisenberg antiferromagnet does indeed have long-range Néel order. All of its ground-state properties as well as long-wavelength excitations are well described by straightforward spin-wave theory. It is reasonable to expect that the antiferromagnet order parameter will reduce its magnitude near a hole. In fact, experiments show that (as an example) in $La_{2-x}Sr_xCuO_4$ magnetic long-range order disappears at a Sr concentration of $x=0.015$, and the material becomes superconducting at about $x=0.05$. The disappearance of Néel order coincides with a dramatic change in the two-dimensional transport properties. The charge carriers in samples that exhibit Néel order are strongly localized, and the electronic conduction is closely similar to that of conventional lightly doped semiconductors. Localization effects are still apparent for samples with intermediate doping levels at low temperature. However, for $T\geqslant 100$ K the samples in this concentration regime exhibit electronic properties closely akin to the normal-state properties of the high-temperature superconductors. Thus, up to the transition regime is an ideal testing ground for the role of magnetic fluctuations in the normal state of the cuprate material. So that investigation of the evolving process of magnetic properties with increasing doping is clearly of great interest. We start our study of the magnetic properties of the t-J model with finite dopant density from the sublattice magnetization at zero temperature.

From Eq. (20), we have

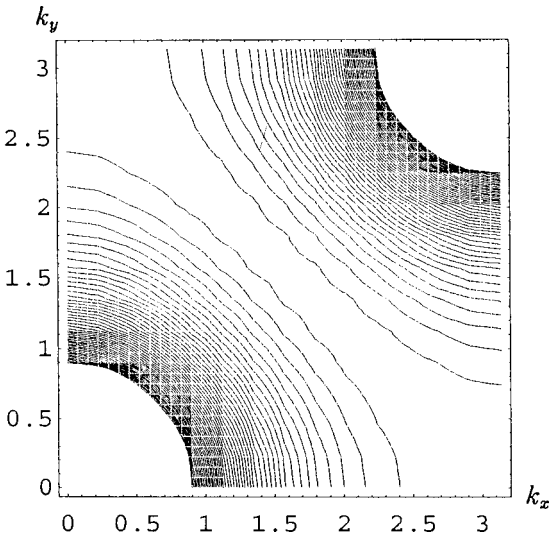

FIG. 7. Hole dispersion contours plotted in the Brillouin zone, for a 2D square lattice with lattice parameter $a=1$, for doping concentration ($\langle f^{\dagger}f\rangle=$)0.001, for $t=1$, $J=0.3$.

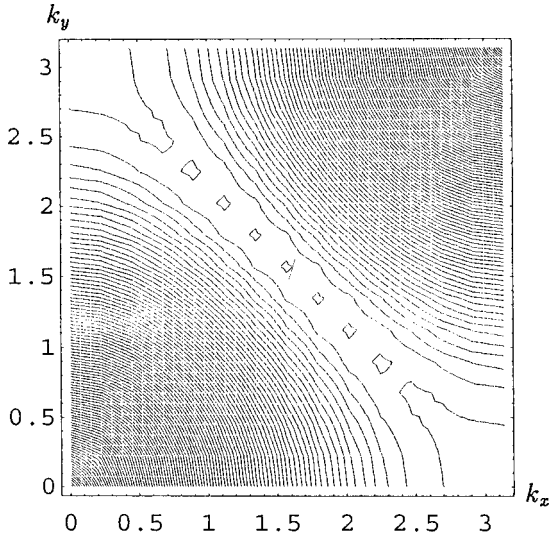

FIG. 9. Hole dispersion contours plotted in the Brillouin zone, for a 2D square lattice with lattice parameter $a=1$, for doping concentration ($\langle f^{\dagger}f\rangle=$)0.01, for $t=1$, $J=0.3$.

$$\langle\langle X^{\uparrow\downarrow}_{\mathbf{j}_1};X^{\downarrow\uparrow}_{\mathbf{k}_1}\rangle\rangle=\frac{2\langle S^3\rangle}{N}\sum_{\mathbf{k}}e^{i\mathbf{k}\cdot(\mathbf{j}_1-\mathbf{k}_1)}\frac{1}{E_s^2-E_h^2}\left[\frac{2t^2z\langle f^\dagger f\rangle-J\langle S^3\rangle zE_h-E_h^2}{E-E_h}+\frac{2t^2z\langle f^\dagger f\rangle+J\langle S^3\rangle zE_h-E_h^2}{E+E_h}\right.$$
$$\left.+\frac{-2t^2z\langle f^\dagger f\rangle+J\langle S^3\rangle zE_s+E_s^2}{E-E_s}+\frac{-2t^2z\langle f^\dagger f\rangle-J\langle S^3\rangle zE_s+E_s^2}{E+E_s}\right]. \tag{22}$$

From the analytical properties of the Green's functions, it follows that the correlation function $\langle X^{\downarrow\uparrow}_{\mathbf{j}1}X^{\uparrow\downarrow}_{\mathbf{j}1}\rangle$ can be obtained from the equation

$$\langle X^{\downarrow\uparrow}_{\mathbf{j}_1}X^{\uparrow\downarrow}_{\mathbf{j}_1}\rangle=i\frac{\langle S^3\rangle}{\pi N}\sum_{\mathbf{k}}\frac{1}{E_s^2-E_h^2}\left\{\int_{-\infty}^{\infty}\frac{d\omega}{e^{\beta\omega}+1}\left[(2t^2z\langle f^\dagger f\rangle-J\langle S^3\rangle zE_h-E_h^2)\left(\frac{1}{\omega-E_h+i0^+}-\frac{1}{\omega-E_h-i0^+}\right)+(2t^2z\langle f^\dagger f\rangle\right.\right.$$
$$\left.+J\langle S^3\rangle zE_h-E_h^2)\left(\frac{1}{\omega+E_h+i0^+}-\frac{1}{\omega+E_h-i0^+}\right)\right]+\int_{-\infty}^{\infty}\frac{d\omega}{e^{\beta\omega}-1}\left[(-2t^2z\langle f^\dagger f\rangle+J\langle S^3\rangle zE_s+E_s^2)\right.$$
$$\left.\left.\times\left(\frac{1}{\omega-E_s+i0^+}-\frac{1}{\omega-E_s-i0^+}\right)+(-2t^2z\langle f^\dagger f\rangle-J\langle S^3\rangle zE_s+E_s^2)\left(\frac{1}{\omega+E_s+i0^+}-\frac{1}{\omega+E_s-i0^+}\right)\right]\right\}$$
$$=\frac{2\langle S^3\rangle}{N}\sum_{\mathbf{k}}\frac{1}{E_s^2-E_h^2}\left[\frac{2t^2z\langle f^\dagger f\rangle-J\langle S^3\rangle zE_h-E_h^2}{e^{\beta E_h}+1}+\frac{2t^2z\langle f^\dagger f\rangle+J\langle S^3\rangle zE_h-E_h^2}{e^{-\beta E_h}+1}\right.$$
$$\left.+\frac{-2t^2z\langle f^\dagger f\rangle+J\langle S^3\rangle zE_s+E_s^2}{e^{\beta E_h}-1}+\frac{-2t^2z\langle f^\dagger f\rangle-J\langle S^3\rangle zE_s+E_s^2}{e^{-\beta E_s}-1}\right]\equiv 2\langle S^3\rangle\Phi, \tag{23}$$

where

$$\Phi\equiv\frac{1}{N}\sum_{\mathbf{k}}\frac{1}{E_s^2-E_h^2}\left[\frac{2t^2z\langle f^\dagger f\rangle-J\langle S^3\rangle zE_h-E_h^2}{e^{\beta E_h}+1}+\frac{2t^2z\langle f^\dagger f\rangle+J\langle S^3\rangle zE_h-E_h^2}{e^{-\beta E_h}+1}+\frac{-2t^2z\langle f^\dagger f\rangle+J\langle S^3\rangle zE_s+E_s^2}{e^{\beta E_s}-1}\right.$$
$$\left.+\frac{-2t^2z\langle f^\dagger f\rangle-J\langle S^3\rangle zE_s+E_s^2}{e^{-\beta E_s}-1}\right]. \tag{24}$$

From Eq. (7), we obtain

$$\langle S^3\rangle=\frac{1}{2}(1-\langle f^\dagger f\rangle)-\langle X^{\downarrow\uparrow}X^{\uparrow\downarrow}\rangle. \tag{25}$$

And then,

$$\langle S^3\rangle=\frac{1}{2}(1-\langle f^\dagger f\rangle)-2\langle S^3\rangle\Phi. \tag{26}$$

Therefore, we can write $\langle S^3\rangle$ formally as

$$\langle S^3\rangle=\frac{1-\langle f^\dagger f\rangle}{2(1+2\Phi)}. \tag{27}$$

In principle, all of the interested physical results can be obtained by solving the above equation. This is one of the most advantageous features of the Green's-function approach as in the case of magnetism.[20,21]

At zero temperature, the function Φ is of the form

$$\Phi_0=\frac{1}{N}\sum_{\mathbf{k}}\left[J\langle S^3\rangle z\frac{E_s+E_h}{E_s^2-E_h^2}-\frac{E_s^2+E_h^2}{E_s^2-E_h^2}+\frac{4t^2z\langle f^\dagger f\rangle}{E_s^2-E_h^2}\right]. \tag{28}$$

In the case of low doping concentration,

$$\Phi_0=\frac{1}{N}\sum_{\mathbf{k}}\left[\frac{1}{\sqrt{1-\gamma^2(\mathbf{k})}}-1+\frac{4t^2z\langle f^\dagger f\rangle}{J^2\langle S^3\rangle^2z^2}\frac{1}{1-\gamma^2(\mathbf{k})}\right]. \tag{29}$$

At exact half-filling, the function Φ_0 reduces as

$$\Phi_0=\frac{1}{N}\sum_{\mathbf{k}}\left(\frac{1}{\sqrt{1-\gamma^2(\mathbf{k})}}-1\right). \tag{30}$$

For the cubic lattice,[35]

$$C''=\frac{2}{N}\sum_{\mathbf{k}}\frac{1}{1-\gamma^2(\mathbf{k})}=1.516.$$

At zero temperature, we get

$$\Phi_0=0.078+0.505\frac{1}{(\langle S^3\rangle)^2}\left(\frac{t}{J}\right)^2\langle f^\dagger f\rangle. \tag{31}$$

From Eqs. (27) and (31), we obtain the average magnetization (for low dopant density) per lattice as

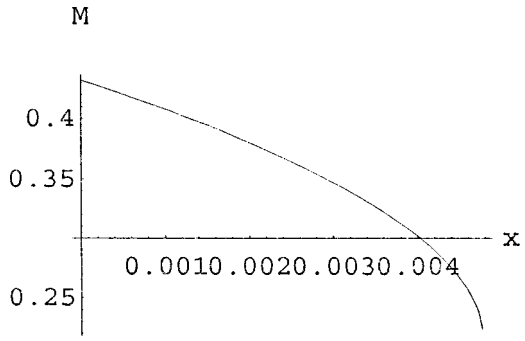

FIG. 10. Sublattice magnetization $M(\equiv\langle S^3\rangle)$ as a function of doping concentration $x(\equiv\langle f^\dagger f\rangle)$, for $t=1$, $J=0.3$.

$$\langle S^3\rangle_0 = 0.216\left[1-\langle f^\dagger f\rangle + \sqrt{(1-\langle f^\dagger f\rangle)^2 - 18.681\left(\frac{t}{J}\right)^2\langle f^\dagger f\rangle}\right]. \quad (32)$$

Expanding the expression of magnetization in terms of the doping concentration ($\langle f^\dagger f\rangle$), we find that the first term recovers the result for the antiferromagnetism.[21] And the second part comes from the linear effect of the doping on the antiferromagnetic long-range order. It is the third term that is remarkable, which is very sensitive to the doping. Although in the low doping case, this term cannot be ignored at all. In Fig. 10, we give a plot of the doping-dependent magnetization at zero temperature. It shows that the sublattice magnetization is reduced rapidly with increasing dopant density. It is in good agreement with neutron-scattering experiments in high-temperature cuprate materials.

V. MAGNETIZATION AT LOW TEMPERATURES

It is within our expectations that the temperature dependence of the sublattice magnetization for undoped high-temperature cuprate materials is in quantitative agreement with a spin-wave analysis of a Heisenberg Hamiltonian. Years ago, in neutron-scattering experiments for $La_2CuO_{4+\delta}$ and $YBa_2Cu_3O_{6+x}$, Keimer *et al.*[19] found that the temperature dependence of the sublattice magnetization for the hole-doped samples evolves continuously with dopant concentration, the sublattice magnetization curve first flattens and ultimately becomes reentrant at low temperatures. A possible explanation for this feature may be that the localized holes frustrate the superexchange interaction between the Cu spins and hence lead to a rapid suppression of the Néel temperature T_N. However, by contrast, such behavior is observed neither in the data for the diluted samples nor in equivalent data for the $Pr_{2-x}Ce_xCuO_4$ system. Thus, frustration is presumably not a major factor in the destruction of long-range antiferromagnetism in the compounds doped with excess electrons. It is clearly important to find other explanations for this strange behavior of high-temperature superconductors at low temperatures. In the follows, we calculate the sublattice magnetization at low temperatures using the t-J model.

For low temperatures, the summation over the momentum wave space involved in the calculation of Φ in the above section can be replaced by the integration

$$\begin{aligned}\Phi &= \frac{1}{N}\sum_{\mathbf{k}}\frac{1}{E_s^2-E_h^2}\left[-\frac{2t^2z\langle f^\dagger f\rangle - J\langle S^3\rangle zE_h - E_h^2}{e^{-\beta E_h}+1} + \frac{2t^2z\langle f^\dagger f\rangle + J\langle S^3\rangle zE_h - E_h^2}{e^{-\beta E_h}+1} + (2t^2z\langle f^\dagger f\rangle - J\langle S^3\rangle zE_h - E_h^2)\right.\\ &\left. - \frac{-2t^2z\langle f^\dagger f\rangle + J\langle S^3\rangle zE_s + E_s^2}{e^{-\beta E_s}-1} + \frac{-2t^2z\langle f^\dagger f\rangle - J\langle S^3\rangle zE_s + E_s^2}{e^{-\beta E_s}-1} - (-2t^2z\langle f^\dagger f\rangle + J\langle S^3\rangle zE_s + E_s^2)\right]\\ &= \Phi_0 - \frac{2}{N}\sum_{\mathbf{k}}\frac{J\langle S^3\rangle zE_h}{E_s^2-E_h^2}\left(1-\frac{1}{e^{-\beta E_h}+1}\right) + \frac{2}{N}\sum_{n=1}^{\infty}\sum_{\mathbf{k}}\frac{1}{E_s^2-E_h^2}J\langle S^3\rangle zE_s e^{-\beta nE_s}. \end{aligned} \quad (33)$$

In the case of small doping, we have

$$\Phi = \Phi_0 + \frac{2}{N}\sum_{n=1}^{\infty}\sum_{\mathbf{k}}\frac{1}{\sqrt{1-\gamma^2(\mathbf{k})}}e^{-\beta nJ\langle S^3\rangle z\sqrt{1-\gamma(\mathbf{k})}} - \frac{2}{N}\sum_{\mathbf{k}}\frac{1}{1-\gamma^2(\mathbf{k})}\frac{2t^2z\langle f^\dagger f\rangle}{J^2\langle S^3\rangle^2z^2}\frac{1}{e^{\beta(2t^2z\langle f^\dagger f\rangle/J\langle S^3\rangle z)}+1}. \quad (34)$$

Therefore, we have

$$\Phi = \Phi_0 + \frac{\sqrt{3}\zeta(2)}{24\pi^2}\left(\frac{kT}{J\langle S^3\rangle}\right)^2 - 0.505\frac{1}{\langle S^3\rangle^2}\left(\frac{t}{J}\right)^2\langle f^\dagger f\rangle\frac{1}{e^{\beta(2t^2z\langle f^\dagger f\rangle/J\langle S^3\rangle x)}+1}, \quad (35)$$

and, so that

$$\langle S^3\rangle = \langle S^3\rangle_0 - \frac{\sqrt{3}\zeta(2)}{6\pi^2(1-\langle f^\dagger f\rangle)}\left(\frac{kT}{J}\right)^2 + 2.02\left(\frac{t}{J}\right)^2\frac{\langle f^\dagger f\rangle}{(1-\langle f^\dagger f\rangle)}\frac{1}{e^{\beta(4t^2\langle f^\dagger f\rangle/J)}+1}. \quad (36)$$

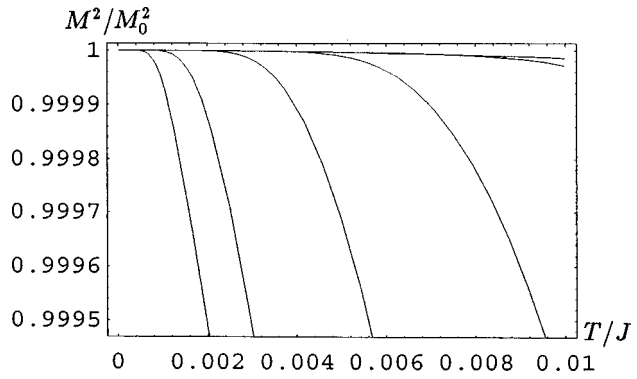

FIG. 11. Square of the sublattice magnetization M^2/M_0^2 as a function of the temperature T/J, for different doping concentrations (starting from below $\langle f^\dagger f\rangle = 0.0001$, 0.0002, 0.0005, 0.001, 0.002, 0.003).

The doping effect of the temperature-dependent terms in the above equation is really surprising to compare with the theory of the magnon-hole interaction,[36] which is a natural generalization of the Dyson-Oguchi theory for the antiferromagnetism.[37] Sometimes the dopings do not destroy but enhance the half-filled ground state at low temperatures. It is a nonperturbative behavior of the t-J model, which cannot be detected by any perturbative method. Indeed, the result is in good agreement with the neutron-scattering experiments:[19] the order-parameter curves of the sublattice magnetization with increasing doping first flattens and ultimately exhibits reentrant behavior at low temperatures. Figure 11 shows the magnetization at low temperatures for different doping concentrations from 0.0001 to 0.003. Of course, in the case of zero doping, we recover all of the results for the antiferromagnetism.

VI. ANTIFERROMAGNETIC-METALLIC PHASE TRANSITION AND NÉEL TEMPERATURES

Undoped cuprate materials are described by the two-dimensional Heisenberg Hamiltonian, and a small coupling between the CuO_2 layers leads to the formation of a three-dimensional Néel-ordered state. The only phase transition for the undoped parent compounds is the antiferromagnetic-paramagnetic one, which occurred at Néel temperature T_{N0}. Several analytical approaches (generalized Schwinger-boson mean-field theory,[38] spin-wave theory[39]) were developed to discuss this phase transition and the dependence of Néel temperature on the anisotropy parameter. However, the phase diagram of the high-temperature superconductors shows the presence of an antiferromagnetic-metallic phase transition at Néel temperature T_N, which is seriously dependent on the dopant density. The influence of dopant on the Néel temperature was investigated extensively by neutron-scattering and muon-spin resonance experiments. The Néel temperature is heavily suppressed by doping in any sample. The disappearance of Néel order coincides with a dramatic change in the two-dimensional transport properties. The charge carriers in samples that exhibit Néel order are strongly localized, and the electronic conduction is closely similar to that of conventional lightly doped semiconductors. Localization effects are apparent at low temperature. However, for high temperatures the samples exhibit electronic properties closely akin to the normal-state properties. Thus, to gain insight into the antiferromagnetic-metallic phase transition and the doping effect of Néel temperature is clearly interested.

To evaluate the Néel temperature, in the low doping case, we expand in Laurant series the function Φ for very small $\langle S^3\rangle$. And then

$$\Phi = \frac{1}{N}\sum_{\mathbf{k}} \frac{1}{E_s^2 - E_h^2}\left[(2t^2 z\langle f^\dagger f\rangle - J\langle S^3\rangle z E_h - E_h^2)\left(\frac{1}{2} - \frac{\beta E_h}{4}\right) + (2t^2 z\langle f^\dagger f\rangle + J\langle S^3\rangle z E_h - E_h^2)\left(\frac{1}{2} + \frac{\beta E_h}{4}\right) + (-2t^2 z\langle f^\dagger f\rangle + J\langle S^3\rangle z E_s + E_s^2)\left(\frac{1}{\beta E_s} - \frac{1}{2} + \frac{\beta E_s}{12}\right) + (-2t^2 z\langle f^\dagger f\rangle - J\langle S^3\rangle z E_s + E_s^2)\left(-\frac{1}{\beta E_s} - \frac{1}{2} - \frac{\beta E_s}{12}\right)\right] \tag{37}$$

$$= \frac{2}{N}\sum_{\mathbf{k}} \frac{1}{E_s^2 - E_h^2}\left[J\langle S^3\rangle z E_s \frac{1}{\beta E_s} - \left(-2t^2 z\langle f^\dagger f\rangle + \frac{E_h^2 + E_s^2}{2}\right) + J\langle S^3\rangle z(3E_h^2 + E_s^2)\frac{\beta}{12}\right]. \tag{38}$$

A straightforward calculation allows us to write Φ as

$$\Phi = \sum_{\mathbf{k}} \frac{1}{1-\gamma^2(\mathbf{k})}\frac{kT}{J\langle S^3\rangle z} - \left[\frac{1}{2} - \frac{2t^2 z\langle f^\dagger f\rangle}{J^2\langle S^3\rangle^2 z^2}\sum_{\mathbf{k}} \frac{1}{1-\gamma^2(\mathbf{k})}\right] + J\langle S^3\rangle z \frac{1}{12kT}. \tag{39}$$

Equations (27) and (39) imply

$$\langle S^3\rangle = \frac{1-\langle f^\dagger f\rangle}{2(1+2\Phi)} = \frac{1-\langle f^\dagger f\rangle}{4}\left[\frac{C'' kT}{J\langle S^3\rangle z} + \frac{2C'' t^2 z\langle f^\dagger f\rangle}{J^2\langle S^3\rangle^2 z^2} + \frac{J\langle S^3\rangle z}{12kT}\right]^{-1} \tag{40}$$

or

$$\frac{Jz}{12kT}(\langle S^3\rangle)^3 - 3\left(\frac{1-\langle f^\dagger f\rangle}{12} - \frac{C'' kT}{3Jz}\right)\langle S^3\rangle + \frac{2C'' t^2 z\langle f^\dagger f\rangle}{J^2 z^2} = 0. \tag{41}$$

Then, we obtain an expression for the sublattice magnetization near the Néel temperature

$$\langle S^3\rangle=\frac{1}{2^{1/3}}\left[-\frac{24C''t^2z\langle f^\dagger f\rangle}{J^3z^3}\,kT+\sqrt{\left(\frac{24C''t^2z\langle f^\dagger f\rangle}{J^3z^3}\,kT\right)^2-4\left(\frac{1-\langle f^\dagger f\rangle}{Jz}\,kT-\frac{4C''}{J^2z^2}\,k^2T^2\right)^3}\right]^{1/3}e^{2\pi i/3}$$
$$+\frac{1}{2^{1/3}}\left[-\frac{24C''t^2z\langle f^\dagger f\rangle}{J^3z^3}\,kT-\sqrt{\left(\frac{24C''t^2z\langle f^\dagger f\rangle}{J^3z^3}\,kT\right)^2-4\left(\frac{1-\langle f^\dagger f\rangle}{Jz}\,kT-\frac{4C''}{J^2z^2}\,k^2T^2\right)^3}\right]^{1/3}e^{4\pi i/3}. \tag{42}$$

In the case of zero doping ($\langle f^\dagger f\rangle=0$), the above equation reduces to the familiar form of the sublattice magnetization for the antiferromagnetism,

$$\langle S^3\rangle=\frac{1}{2}\sqrt{\frac{3}{C''}\frac{T}{T_{N0}}\left(1-\frac{T}{T_{N0}}\right)}, \tag{43}$$

where $kT_{N0}\equiv Jz/4C''$ is the Néel temperature at half-filling.

The physical constraint of quantity $\langle S^3\rangle$ being a real value, i.e., $\langle S^3\rangle^*=\langle S^3\rangle$, implies

$$\left(\frac{24C''t^2z\langle f^\dagger f\rangle}{J^3z^3}\,kT\right)^2-4\left(\frac{1-\langle f^\dagger f\rangle}{Jz}\,kT-\frac{4C''}{J^2z^2}\,k^2T^2\right)^3\leqslant 0. \tag{44}$$

The following equation is satisfied by the Néel temperature T_N:

$$(kT_N)^{4/3}-\frac{Jz(1-\langle f^\dagger f\rangle)}{4C''}\,(kT_N)^{1/3}+\frac{(12C''t^2z\langle f^\dagger f\rangle)^{2/3}}{4C''}=0. \tag{45}$$

Then, we get an expression of the Néel temperature,

$$kT_N=\frac{Jz(1-\langle f^\dagger f\rangle)}{4C''}-\left[\frac{(3t^2z\langle f^\dagger f\rangle)^2}{Jz}\right]^{1/3}. \tag{46}$$

Above the transit temperature region ($T>T_N$), $\langle S^3\rangle$ has no definite value. Unlike the antiferromagnetism case, it is not permissible to arrive at the paramagnetic phase, where $\langle S^3\rangle=0$. This fact is in agreement with the phase diagram of the realistic high-temperature superconductors, where above the antiferromagnetic phase is the metallic, but not the paramagnetic phase.

It is clear that the Néel temperature is heavily dependent on the doping concentration $\langle f^\dagger f\rangle$. From Fig. 12, we know that, at about $\langle f^\dagger f\rangle=0.01$, the Néel temperature is already reduced to zero. This is in agreement with experiments on high-temperature superconductors.

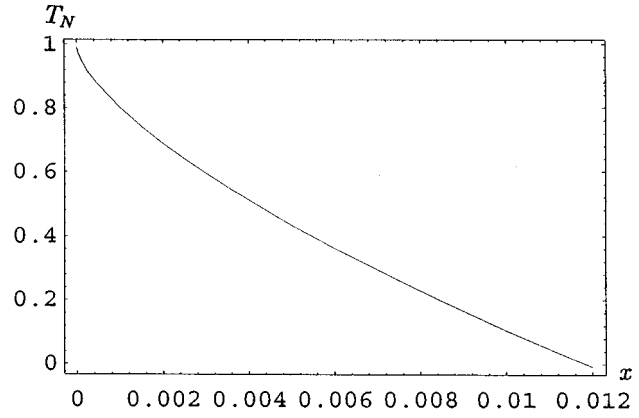

FIG. 12. Néel temperature as a function of doping concentrations, for a 3D cubic lattice with lattice parameter $a=1$, for $J=1$, $J/t=0.3$.

VII. CONCLUDING REMARKS

The magnetism in undoped high-temperature superconductors is now quite well understood. The system of interacting localized Cu^{2+} spins is well described by the two-dimensional Heisenberg Hamiltonian, and a small coupling between the CuO_2 layers leads to the formation of a three-dimensional Néel-ordered state. It is therefore clearly of great interest to investigate in detail the crossover from the rather conventional local moment system at zero doping to the electronic state that forms the basis for high-temperature superconductivity. Many theorists strongly argued that the appropriate model for high-temperature superconductivity is the single-band Hubbard model or its equivalence at the strong-coupling limit, the t-J model. The Hubbard model and the t-J model are believed to represent the gross features of the electronic behavior of the new materials.

In this paper, we discussed magnetic properties of the high-temperature superconductors from zero to intermediate doping levels in a whole temperature range by making use of the t-J model and quantum field theory. The quasiparticle picture, and in particular, dispersion relations for holons and renormalized spinons were presented. Results show massless spin-wave excitations at half-filling. The effect of doping opens a gap in the spectrum. The study for motions of a few holes in an antiferromagnetic background has been an important topic in the study of the high-temperature superconductivity for long time. To gain some intuition on the behavior of holes doped into an antiferromagnet, one always starts with the study of just one hole. The physics of a hole arises from a competition between the superexchange energy lost near the hole and its kinetic energy. The effects of a so-called string linear potential strongly influence the physics of holes in antiferromagnets. For the particular case of one hole in an antiferromagnet, an analytical approach have been developed that gives results in good agreement with the exact diagonalization predictions. Unfortunately, an extension of this approach to a finite density of holes is difficult. We have obtained a general expression for the dispersion relation of holons. Its total bandwidth W provides information about the renormalization effects caused by the spin waves that are created and absorbed while the hole propagates. The bandwidth seems proportional to J/t. This result is in good agreement with other calculations and numerical simulations for a hole in antiferromagnets. The hole dispersion curve is in agreement with numerical ones using a Green's-function Monte Carlo method and the Born approximation. An interesting feature is the degeneracy between momentum **k**

$=(\pi/2,\pi/2)$ and $\mathbf{k}=(0,\pi)$, $(\pi,0)$. Analyzed from the point of view of the Hubbard model, this is not surprising, since in the noninteracting limit both momenta belong to the Fermi surface, thus at least at weak coupling, only a tiny splitting in energy is expected. However, the Born approximation and numerical simulation using a Green's-function Monte Carlo method show a small difference in energy between $\mathbf{k}=(\pi/2,\pi/2)$ and $\mathbf{k}=(0,\pi)$, $(\pi,0)$. According to Dagotto, Nazarenko, and Boninsegni,[40] it is a small fraction of the difference forming the basis for a possible explanation of the behavior of the Hall coefficient with temperature in the high-temperature superconductors.

Experiments show that the disappearance of Néel order coincides with a dramatic change in the two-dimensional transport properties. Localization effects are still apparent for samples with intermediate doping at low temperature. However, for high temperature the samples in this concentration regime exhibit electronic properties closely akin to the normal-state properties of the high-temperature superconductors. Therefore, it is of clearly great interest to investigate the evolving process of the magnetic properties with increasing dopant density. At zero temperature and in the low doping case, we got an expression of the sublattice magnetization, which is seriously dependent on the dopant density explicitly. This shows that the sublattice magnetization is reduced rapidly with increasing doping concentration. It is in agreement with neutron-scattering experiments in high-temperature cuprate materials.

For low temperatures, we arrived at

$$\langle S^3\rangle=\langle S^3\rangle_0-\frac{\sqrt{3}\zeta(2)}{6\pi^2(1-\langle f^\dagger f\rangle)}\left(\frac{kT}{J}\right)^2+2.02\left(\frac{t}{J}\right)^2\frac{\langle f^\dagger f\rangle}{(1-\langle f^\dagger f\rangle)}\frac{1}{e^{\beta(4t^2\langle f^\dagger f\rangle/J)}+1}. \quad (47)$$

The result gives a reasonable explanation for a strange feature of the high-temperature superconductors: the temperature dependence of the sublattice magnetization for the hole-doped samples evolves continuously with dopant concentration, the sublattice magnetization curve first flattens and ultimately becomes reentrant at low temperatures. Sometimes the dopings do not destroy but enhance the half-filled ground state at low temperatures. It is a nonperturbative behavior of the t-J model, which cannot be detected by any perturbative method.

The only phase transition for the undoped parent compounds is an antiferromagnetic-paramagnetic one, which occurred at Néel temperature T_{N0}. However, a phase diagram of the high-temperature superconductors shows the presence of a antiferromagnetic-metallic phase transition at Néel temperature T_N, which is dependent on the dopant density. The influence of the dopant on the Néel temperature was investigated extensively by neutron-scattering and muon-spin resonance. The Néel temperature is heavily suppressed by doping in any sample. An expression for the sublattice magnetization near the Néel temperature was obtained. The physical constraint of quantity $\langle S^3\rangle$ being a real value, deduces an equation satisfied by the Néel temperature T_N. The solution of this equation gives an expression of the Néel temperature, which is a function of dopant density,

$$kT_N=\frac{Jz(1-\langle f^\dagger f\rangle)}{4C''}-\left[\frac{(3t^2z\langle f^\dagger f\rangle)^2}{Jz}\right]^{1/3}.$$

Above the transit temperature region ($T>T_N$), $\langle S^3\rangle$ has no definite value. Unlike the antiferromagnetic case, it is not permissible to arrive at the paramagnetic phase, where $\langle S^3\rangle=0$. This fact is in agreement with the phase diagram of the realistic high-temperature superconductors, where above the antiferromagnetic phase is the metallic, but not the paramagnetic phase.

ACKNOWLEDGMENT

The work was supported by the National Science Foundation of China.

*Electronic address: changz@bepc3.ihep.ac.cn

[1] J. G. Bednorz and K. A. Müller, Z. Phys. B **64**, 189 (1986).
[2] B. Batlogg, Phys. Today **44**(6), 44 (1991).
[3] J. M. Harris, Y. F. Yan, and N. P. Ong, Phys. Rev. B **46**, 14 293 (1992).
[4] A. J. Millis, H. Monien, and D. Pines, Phys. Rev. B **42**, 167 (1990).
[5] N. E. Bickers, D. J. Scalapino, and S. R. White, Phys. Rev. Lett. **62**, 961 (1989).
[6] P. Monthoux, A. Balatsky, and D. Pines, Phys. Rev. Lett. **67**, 3448 (1991).
[7] K. Miyake, S. Schmitt-Rink, and C. M. Varma, Phys. Rev. B **34**, 6554 (1986).
[8] P. Monthoux and D. Pines, Phys. Rev. B **47**, 6069 (1993).
[9] J. Bardeen, L. Cooper, and J. R. Schrieffer, Phys. Rev. **108**, 1175 (1957).
[10] For the review, see for example, P. A. Lee, in *High-Temperature Superconductivity*, edited by K. S. Bedell *et al.* (Addison-Wesley, New York, 1990); Yu Lu, in *Recent Progress in Many-Body Theories Vol. 3*, edited by T. L. Ainsworth *et al.* (Plenum, New York, 1992); E. Dagotto, Rev. Mod. Phys. **66**, 763 (1994).
[11] P. W. Anderson, Science **235**, 1196 (1987).
[12] J. Hubbard, Proc. R. Soc. London, Ser. A **276**, 238 (1963).
[13] A. B. Harris and R. V. Lange, Phys. Rev. **157**, 279 (1967).
[14] W. F. Brinkman and T. M. Rice, Phys. Rev. B **2**, 1324 (1970).
[15] F. C. Zhang and T. M. Rice, Phys. Rev. B **37**, 3759 (1988).
[16] For a review, see W. E. Pickett, H. Krakauer, R. E. Cohen, and D. J. Singh, Science **255**, 46 (1992).
[17] G. Shirane *et al.*, Phys. Rev. Lett. **63**, 330 (1989); J. Rossat-Mignod *et al.*, Physica C **185–189**, 86 (1991).
[18] For a review, see E. Manousakis, Rev. Mod. Phys. **63**, 1 (1991).
[19] B. Keimer *et al.*, Phys. Rev. B **45**, 7430 (1992); B. Keimer *et al.*, *ibid.* **46**, 14 034 (1992).
[20] N. N. Bogolyubov and S. V. Tyablikov, Dokl. Akad. Nauk SSSR **126**, 53 (1959) [Sov. Phys. Dokl. **4**, 604 (1959)].
[21] F. C. Pu, Dokl. Akad. Nauk SSSR **130**, 1244 (1960); **131**, 546 (1960) [Sov. Phys. Dokl. **5**, 128 (1960)]; [**5**, 321 (1960)].
[22] I. Bars and M. Günaydin, Commun. Math. Phys. **91**, 31 (1983).
[23] T. Holstein and H. Primakoff, Phys. Rev. **58**, 1098 (1940); Z. Chang, J. Math. Phys. **37**, 4252 (1996).
[24] S. V. Tyablikov, Ukr. Mat. Zh. **11**, 287 (1959).
[25] P. W. Anderson, Phys. Rev. Lett. **64**, 1839 (1990).

[26] E. Dagotto, A. Moreo, F. Ortolani, D. Poilbanc, and J. Riera, Phys. Rev. B **45**, 10 741 (1992); J. Bonča, P. Prelovšek, and I. Sega, Europhys. Lett. **10**, 87 (1989).
[27] B. Shraiman and E. Siggia, Phys. Rev. Lett. **61**, 467 (1988).
[28] S. Schmitt-Rink, C. M. Varma, and A. E. Ruckenstein, Phys. Rev. Lett. **60**, 2793 (1988).
[29] C. Kane, P. Lee, and N. Read, Phys. Rev. B **39**, 6880 (1989).
[30] Z. Chang, Phys. Rev. B **53**, 1171 (1996).
[31] F. Marsiglio, A. E. Ruckenstein, S. Schmitt-Rink, and C. Varma, Phys. Rev. B **43**, 10 882 (1991); G. Martinez and P. Horsch, *ibid.* **44**, 317 (1991); Z. Liu and E. Manousakis, *ibid.* **44**, 2414 (1991).
[32] S. Trugman, Phys. Rev. B **41**, 892 (1990); P. Prelovšek, I. Sega, and J. Bonča, *ibid.* **42**, 10 706 (1990).
[33] E. Dagotto, R. Joynt, A. Moreo, S. Bacci, and E. Gagliano, Phys. Rev. B **41**, 9049 (1990); D. Poilblanc, T. Ziman, H. J. Schulz, and E. Dagotto, Phys. Rev. B **47**, 14 267 (1993).
[34] Z. Liu and E. Manousakis, Phys. Rev. B **45**, 2425 (1992).
[35] G. N. Watson, Q. J. Math. **10**, 266 (1939); M. Tikson, Natl. Stand. Ref. Data Ser. (U.S., Natl. Bur. Stand.) **50**, 177 (1953).
[36] Z. Chang, Phys. Rev. B **54**, 10 046 (1996).
[37] F. J. Dyson, Phys. Rev. **102**, 1217 (1956); **102**, 1230 (1956); T. Oguchi, *ibid.* **117**, 117 (1960).
[38] B. Keimer *et al.*, Phys. Rev. B **45**, 7430 (1992).
[39] C. M. Soukoulis, S. Datta, and Y. H. Lee, Phys. Rev. B **44**, 446 (1991).
[40] E. Dagotto, A. Nazarenko, and M. Boninsegni, Phys. Rev. Lett. **73**, 728 (1994).